SEMARAK ILMU PUBLISHING

Semarak Engineering Journal

Journal homepage:
https://semarakilmu.my/index.php/sej/index
ISSN: 3036-0145


# Numerical Analysis of Thermal Intensity and NOx Mitigation in Oxy-Methane Combustion: The Strategic Role of $CO_2$ Dilution for CCS Integration

Nur Atiqah Habib[1], Nor Afzanizam Samiran[1,*], Izuan Amin Ishak[1], Rais Hanizam Madon[2], Nik Normunira Mat Hassan[3]

[1] Department of Mechanical Engineering Technology, Faculty of Engineering Technology, Universiti Tun Hussein Onn Malaysia (UTHM) Higher Education Hub Pagoh, KM 1, Jalan Panchor, 84600 Panchor, Johor, Malaysia
[2] Department of Mechanical Technology, Faculty of Mechanical and Manufacturing Engineering, Universiti Tun Hussein Onn Malaysia (UTHM), 86400 Parit Raja, Batu Pahat, Johor, Malaysia
[3] Faculty of Mechanical Engineering, Kompleks Kejuruteraan Tuanku Abdul Halim Mu'adzam Shah, Universiti Teknologi MARA, 40450 Shah Alam, Selangor, Malaysia

**ARTICLE INFO**

***Article history:***
Received 21 February 2026
Received in revised form 2 April 2026
Accepted 10 April 2026
Available online 28 April 2026

***Keywords:***
Oxy-methane combustion, CFD, NOx emissions, Velocity distribution, $CO_2$ dilution, Carbon Capture and Storage (CCS)

**ABSTRACT**

The transition towards oxy–methane combustion is mainly driven by the need to improve $CO_2$ separation for carbon capture and storage (CCS) applications. However, operating with pure oxygen without any form of dilution often results in excessively high flame temperatures, which can significantly promote thermal $NO_x$ formation. In this study, the issue is examined through CFD simulations, focusing on both emission characteristics and thermal behaviour. The modelling framework combines the k–ω SST turbulence model with a mixture fraction PDF approach to compare three combustion environments, namely air combustion, pure oxygen, and a 50% $O_2$ – 50% $CO_2$ oxy-fuel mixture. The numerical model was first validated against reference data, with temperature deviations remaining below 10%, indicating reasonable agreement. The results show that the pure oxygen case produces the highest peak temperature, reaching approximately 1900 K, which is accompanied by a significant increase in NO emissions due to the temperature-sensitive Zeldovich mechanism. When $CO_2$ is introduced as a diluent, the combustion behaviour changes noticeably. The peak temperature decreases to around 1600 K, while NO formation is reduced. This can be linked to the higher heat capacity of $CO_2$ as well as its contribution to radiative heat transfer, both of which help to moderate the combustion process. Further analysis of the velocity field and species distribution (CO, $O_2$, $CO_2$, and $N_2$) suggests that the 50% $O_2$ – 50% $CO_2$ configuration provides a more balanced condition. It maintains flame stability while keeping pollutant emissions at a lower level and, at the same time, produces a $CO_2$-rich exhaust stream that is more suitable for CCS applications. Overall, the findings suggest that $CO_2$ dilution plays a key role in achieving a practical balance between combustion performance, emission control, and sustainability. This highlights its importance in the design of future low-carbon combustion systems.

* *Corresponding author.*
*E-mail address: afzanizam@uthm.edu.my*

https://doi.org/10.37934/sej.14.1.1836

## 1. Introduction

The combustion of oxy-methane has gained increasing academic attention, as the replacement of atmospheric air with pure oxygen enhances the efficiency of methane oxidation while producing $CO_2$-rich exhaust gases that are easier to capture and store through carbon capture and storage (CCS). The reduction of nitrogen dilution decreases the overall volume of flue gas and increases the concentration of $CO_2$, thereby improving the efficiency of $CO_2$ separation and supporting decarbonisation efforts in various sectors, including power generation and metal processing [1-3].

In oxy-fuel combustion of methane, $NO_x$ formation is largely governed by thermal mechanisms. The use of high-purity oxygen increases the adiabatic flame temperature, particularly in the absence of oxidiser dilution by nitrogen, which can promote NO formation through the extended Zeldovich mechanism. Therefore, stricter control of $NO_x$ emissions is essential for the environmental sustainability of oxy-methane systems, as $NO_x$ contributes to photochemical smog, acid deposition, and adverse health effects [4]. Consequently, commonly adopted mitigation strategies aim to minimise peak flame temperatures and reduce high-temperature residence times without compromising combustion stability and efficiency. In the design of low-$NO_x$ oxy-fuel systems, previous studies suggest that the primary objective is to control peak flame temperature while maintaining stable combustion. Key design strategies therefore focus on controlling oxygen concentration, improving fuel–oxidiser mixing, and preventing localised hotspot formation [5].

Existing literature indicates that substantial reductions in $NO_x$ emissions can be achieved through coordinated control of oxidiser composition, equivalence ratio, burner aerodynamics, and dilution or additive strategies. Reducing the oxygen concentration in the oxidiser stream and increasing $CO_2$ dilution can lower flame temperatures and suppress thermal $NO_x$ formation [6]. Operating under stoichiometric or slightly fuel-rich conditions ($\phi$ = 0.9–1.0) can also prevent excessive temperature rises and reduce $NO_x$ formation without significant losses in combustion efficiency [7]. Furthermore, advanced burner configurations, such as staged, multi-port, and vortex designs, can enhance mixing and redistribute heat release, thereby reducing local hotspots and minimising $NO_x$ formation [8]. Thermal diluents such as $H_2O$ and $CO_2$ can lower peak temperatures by several hundred kelvins, leading to significant reductions in $NO_x$ emissions, while specific additives, such as $H_2$, have also been shown to influence NO formation pathways [9].

Computational Fluid Dynamics (CFD) has become an essential tool for studying oxy-methane combustion due to its capability to model coupled transport processes, including turbulent mixing, chemical heat release, radiative and convective heat transfer, and pollutant formation kinetics under controlled operating conditions. This capability is particularly valuable in non-premixed combustion systems, where fuel and oxidiser are introduced separately and the spatial distribution of mixture fraction strongly influences flame structure through turbulence–chemistry interactions and steep gradients in local composition. Consequently, current CFD studies commonly employ either Reynolds-Averaged Navier–Stokes (RANS) or Large Eddy Simulation (LES) turbulence models to analyse flame behaviour and quantify $NO_x$ formation while optimising system design to reduce emissions without compromising thermal efficiency [10].

Accurate modelling of oxy-methane flame behaviour requires appropriate turbulence modelling due to the strong interactions between turbulence and chemical reactions. Although Large Eddy Simulation (LES) provides high-resolution predictions of flame dynamics, transient behaviour, and $NO_x$ formation, it is computationally expensive [11]. In contrast, the k–ω Shear Stress Transport (SST) RANS model offers a practical balance between accuracy and computational cost, making it suitable for steady-state industrial-scale simulations. Once properly validated, the k–ω SST model has been

shown to provide reliable predictions of temperature distribution and $NO_x$ emissions in oxy-fuel combustion systems [11, 12].

Recent advances in computational studies have further strengthened the role of CFD in understanding oxy-fuel combustion behaviour. Several numerical investigations have applied CFD modelling to analyse the thermo-chemical characteristics of oxy-methane combustion under various operating conditions. Jeon et al. investigated the effect of the degree of premixing between fuel and oxidizer on combustion efficiency for highly $CO_2$-diluted methane oxy-flames and methane/air flames in a pressurized micro-mixer combustor. The study reported that the degree of premixing is a critical parameter in determining combustion efficiency for $CO_2$-diluted oxy-flames, with enhanced premixing promoting more efficient combustion, whereas it has a negligible effect on methane/air flames [13]. Daurer et al. evaluated the numerical modeling and combustion characteristics of hydrogen oxy-fuel combustion in a semi-industrial furnace using 3D CFD simulations to analyze turbulence, combustion chemistry, and thermal radiation. The study reported that turbulence modeling dominates the numerical representation of the flame, and that replacing methane with hydrogen increases peak flame temperatures by 400 K and reduces flame length by almost 10%, thereby improving radiative heat transfer [14]. Gu et al. studied the scale-up characteristics of oxy-fuel combustion in circulating fluidized bed (CFB) boilers, ranging from lab-scale to industry-scale, using 3D CFD simulations based on the Eulerian-Lagrangian approach. The study reported that scaling up to a larger oxy-fuel power plant is highly beneficial, as it yields a higher carbon conversion ratio and significantly lowers emissions of CO, NO, and $SO_2$ compared to smaller scales [15]. Kislinger et al. conducted a detailed CFD study coupled with a transient bloom model to investigate oxygen-enriched and partial oxy-fuel combustion in an industrial reheating furnace, utilizing a thermodynamic redistribution method to optimize fuel savings. The study reported that oxygen enrichment to 25 vol% reduced fuel demand and $CO_2$ emissions by 4.8% but more than doubled NO formation, whereas partial oxy-fuel substitution in one combustion zone achieved comparable fuel savings while successfully keeping NOx emissions low [16].

Despite these advances, most existing studies primarily focus on specific oxy-fuel configurations or particular operating conditions. Systematic comparisons between conventional air combustion, pure oxygen combustion, and partially diluted oxy-fuel mixtures remain relatively limited in the literature. Such comparative analyses are important because oxidiser composition strongly influences flame temperature, species formation, and flow dynamics, which ultimately determine combustion stability, pollutant formation, and thermal efficiency. In addition, While the general effects of $CO_2$ dilution on flame temperature are documented, this study distinguishes itself by providing a systematic comparative framework specifically designed for CCS-ready non-premixed systems. By employing the k-$\omega$ SST turbulence model, this research offers a more refined analysis of the spatial trade-offs between thermal intensity and CO oxidation kinetics compared to standard k-$\in$ approaches. Furthermore, the investigation of a specific 50% $O_2$ – 50% $CO_2$ mixture serves as a critical technical baseline for transitioning industrial air-fired systems to high-efficiency carbon-neutral combustion.

In this context, the present study aims to numerically investigate methane combustion under three different oxidiser environments: conventional air, pure oxygen (100% $O_2$), and an oxy-fuel mixture consisting of 50% $O_2$ and 50% $CO_2$. Using CFD simulation, the performance of these oxidisers is compared in terms of temperature distribution, species formation, and flow velocity characteristics within the combustion chamber. The results are expected to provide deeper insight into the influence of oxidiser composition on oxy-methane combustion behaviour and contribute to the development of more efficient low-emission combustion systems.

## 2. Methodology

### *2.1 Burner Geometry*

Figure 1 illustrates the three-dimensional geometry of the single-stage combustor used as the computational domain. The computational domain represents a confined, furnace-scale cylindrical combustion chamber designed for non-premixed combustion studies. The system utilizes a multi-port burner configuration consisting of a central fuel injector surrounded by six peripheral oxidizer inlets to promote turbulent mixing. The combustor consists of a cylindrical chamber with a centrally located fuel injector and surrounding oxidiser inlets. The oxidiser streams (air, 100% $O_2$, or 50% $O_2$–50% $CO_2$) enter through ports around the fuel injector, creating crossflow interactions that promote turbulent mixing within the chamber. This injector arrangement enhances the interaction between the fuel jet and oxidiser streams, facilitating effective mixing prior to combustion. The defined geometry also provides the reference coordinates for extracting axial and sectional data during post-processing of the simulation results. The chamber has a total length of 2000 mm and a diameter of approximately 700 mm, while the fuel injector diameter is 20 mm. These dimensions influence the bulk flow velocity, jet penetration, and mixing behaviour inside the combustor. The relatively long combustor length mimics a laboratory-scale horizontal furnace and also allows sufficient space for flame development and stabilisation providing sufficient residence time for complete methane oxidation and NOx formation analysis along the axial direction.

along the axial direction. Maintaining the same geometric configuration for all simulations ensures that the observed differences in combustion characteristics are primarily attributed to variations in the oxidiser composition rather than geometric effects.

For quantitative analysis, the temperature, velocity, and species distributions were extracted along the combustor centreline. The centreline location was selected as it represents the primary reaction zone where the interaction between the fuel jet and oxidiser streams is most pronounced, allowing a clearer assessment of combustion development along the axial direction.

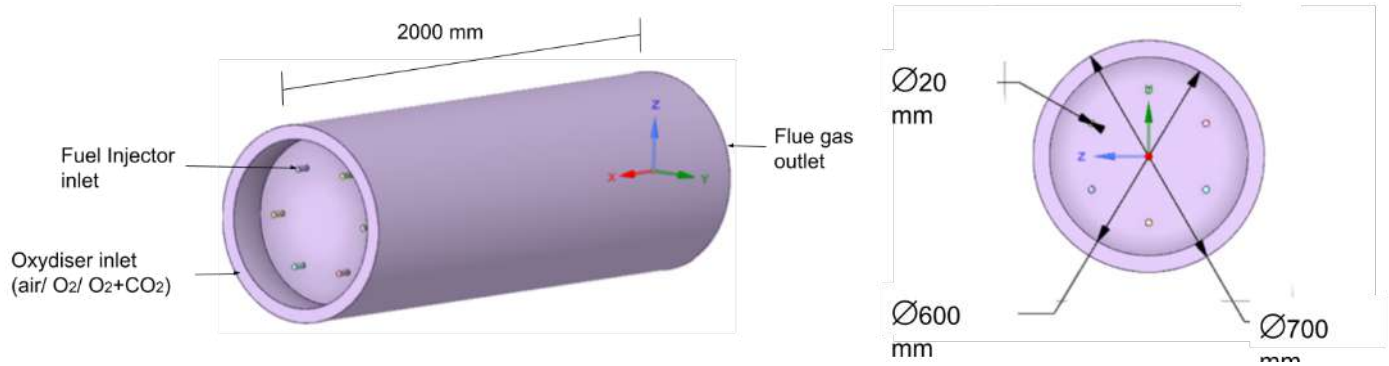


**Fig. 1.** Geometric configuration and primary dimensional parameters of the computational domain (L = 2000 mm, $\phi \approx 700$ mm), illustrating the detailed arrangement of fuel and oxidizer injection ports for CFD model development.

### *2.2 Mesh Generation*

A highly uniform mesh was used to discretise the computational domain with a global element size of 30mm. This option was based on an earlier mesh-sensitivity investigation, to balance accuracy, convergence, and the cost of the coupled reacting-flow simulations of momentum, energy (and species) equations. This resolution is enough to define the main flow and thermal properties, in

particular, the axial temperature development and pressure variation. Mesh quality control has been obtained through imposing reasonable skewness and smooth gradation of cell size, reducing the discretisation error, and enhancing solver stability. As shown in Figure 2, the mesh is uniform both in the axial and radial direction, which allows a consistent representation of global flame structure and heat-release behaviour, and allows a reasonable computational cost to be used in this study.

**Fig. 2.** Discretised computational domain illustrating the uniform structural mesh in both axial and radial directions. A global element size of 30 mm was implemented to ensure numerical accuracy while maintaining computational feasibility for the coupled reacting-flow simulations.

### *2.2 Governing Equation*

The numerical modelling of oxy–methane combustion was performed by solving the governing equations of mass, momentum, energy, and chemical species conservation. These equations describe the transport of mass, momentum, energy, and species within the computational domain. The temperature field predicted from the energy equation plays a significant role in determining the reaction rate and the formation of nitrogen oxides ($NO_x$). Meanwhile, the species transport equations describe the mixing process between methane fuel and oxygen oxidiser as well as the formation of combustion products.

For the non-premixed combustion configuration used in this study, the interaction between methane fuel and oxygen oxidiser was modelled using the mixture fraction probability density function (PDF) approach available in ANSYS Fluent. This approach describes the combustion process based on the turbulent mixing between fuel and oxidiser streams.

To improve the prediction of flame temperature, radiative heat transfer was incorporated into the simulation. The formation of $NO_x$ emissions was evaluated using temperature-dependent sub-models available in ANSYS Fluent. All governing equations were solved simultaneously using the finite volume method to predict the flow behaviour, combustion characteristics, flame structure, and pollutant formation within the combustion chamber. The conservation of mass within the computational domain is expressed by the continuity equation as follows:

$$\frac{\partial \rho}{\partial t} + \nabla \cdot (\rho u) = 0 \quad (1)$$

where $\rho$ represents the fluid density and $u$ denotes the velocity vector. This equation ensures that the rate of mass accumulation in a control volume is equal to the net mass flux entering and leaving the control volume, thereby satisfying the principle of mass conservation throughout the flow domain. The momentum conservation equation describes the transport of momentum within the fluid and is written as:

$$\frac{\partial (\rho u)}{\partial t} + \nabla \cdot (\rho uu) = -\nabla p + \nabla \cdot (\tau) + \rho g \quad (2)$$

Where p is the static pressure, $\tau$ is the viscous stress tensor, and g represents the gravitational acceleration. This equation accounts for the effects of pressure gradients, viscous forces, and body forces acting on the fluid. Solving the momentum equation enables the prediction of velocity and pressure distributions within the combustion chamber. The conservation of energy in the combustion system is governed by the following equation:

$$\frac{\partial (\rho h)}{\partial t} + \nabla \cdot (\rho uh) = \nabla \cdot (k_{eff} \nabla T) + S_h + S_r \quad (3)$$

where h is the sensible enthalpy, T is the temperature, and $k_{eff}$ represents the effective thermal conductivity. The terms $S_h$ and $S_r$ denote the volumetric heat source due to chemical reactions and the radiative heat source, respectively. This equation accounts for the transport of thermal energy through convection and conduction, as well as heat generation resulting from combustion reactions. The energy equation is essential for predicting the temperature distribution within the combustion region. For non-premixed combustion modelling, the interaction between fuel and oxidiser is described using a conserved scalar known as the mixture fraction Z. The mixture fraction represents the local mass fraction originating from the fuel stream. The transport equation for the mixture fraction is expressed as:

$$\frac{\partial (\rho Z)}{\partial t} + \nabla \cdot (\rho uZ) = \nabla \cdot (D_{eff} \nabla Z) \quad (4)$$

Where $Z$ represents the mixture fraction and $D_{eff}$ is the effective diffusion coefficient. The mixture fraction varies between 0 and 1, where $Z = 0$ corresponds to the pure oxidiser stream and $Z = 1$ corresponds to the pure fuel stream. Thermochemical properties such as temperature and species concentrations are obtained from a pre-computed probability density function (PDF) table that accounts for the effects of turbulent fluctuations on the combustion process. Radiative heat transfer plays an important role in high-temperature combustion systems and significantly influences the flame temperature distribution. In this study, radiation heat transfer was modelled using the Discrete Ordinates (DO) radiation model. The radiative transfer equation (RTE) can be expressed as:

$$\nabla . (I\vec{s}) + (a + \sigma_s) I = an^2 \frac{\sigma T^4}{\pi} \quad (5)$$

where $I$ represents radiation intensity, $a$ is the absorption coefficient, $\sigma_s$ is the scattering coefficient, and $\vec{s}$ is the radiation direction vector. For the chemical reaction modeling, the Equilibrium Chemistry approach was utilized within the Non-Premixed Combustion framework. This model assumes that the chemical reactions are fast enough to reach equilibrium at the molecular level. The PDF table was generated considering a multi-component fuel stream consisting of $CH_4$, $O_2$ and trace amounts of $N_2$, and $CO_2$ by mole fraction. The effect of turbulent fluctuations on the chemistry was accounted for using a $\beta$-Probability Density Function (PDF)

### *2.3 Boundary Condition*

The primary oxidiser inlets were specified as mass flow inlet boundary conditions in the present study. The mass flow rates were prescribed based on the operating conditions, while the inlet

temperature for both streams was fixed at 300 K. Turbulent inflow conditions were imposed at both inlets with a turbulence intensity of 10% and a turbulent viscosity ratio of 10. Methane was introduced through a separate mass flow inlet, allowing precise control of the fuel injection rate under non-premixed combustion conditions. This configuration ensures that the mixing between methane fuel and oxygen oxidiser occurs within the combustion chamber. The selection of a 50% $O_2$ – 50% $CO_2$ dilution ratio was established as a representative baseline case for high-dilution oxy-fuel combustion. This specific ratio is frequently cited in literature as a critical threshold that balances flame stability with the production of a high-purity $CO_2$ stream suitable for Carbon Capture and Storage (CCS). While different dilution ratios would further influence the thermal gradients, this 50% configuration serves as a 'worst-case' scenario for moderate combustion intensity, providing a clear technical benchmark for the transition from air-fired to $CO_2$-diluted systems.

The outlet boundary was defined as a pressure outlet with a gauge pressure of 0 Pa, enabling a stable outflow of combustion products from the domain. All combustor walls were assumed to be adiabatic, corresponding to zero heat flux conditions. Therefore, external heat losses were neglected, allowing the analysis to focus on intrinsic combustion characteristics and $NO_x$ formation within the system.

**Table 1**
Boundary Conditions in The Numerical Simulation

| No. | Boundary Name | Boundary Type | Specification |
|---|---|---|---|
| 1 | Primary Oxidiser Inlet | Mass Flow Inlet | $\dot{m}=9.545\times10^{-4}$ kg/s ,T=300K |
| 2 | Fuel Inlet (Methane) | Mass Flow Inlet | $\dot{m}=1.167\times10^{-4}$ kg/s |
| 3 | Outlet | Pressure Outlet | Gauge Pressure = 0 Pa |

The boundary conditions applied in the numerical simulation are summarised in Table 1. Appropriate boundary types and operating parameters were assigned to ensure numerical stability and accurate prediction of the flow, thermal, and chemical behaviour of the non-premixed oxy–methane combustion system.

### *2.4 Grid Independence Analysis and Validation of Numerical Model*

To ensure the numerical accuracy and reliability of the simulation, a grid independence test was performed. Five different mesh densities were evaluated, ranging from approximately 140,000 to 2,200,000 elements. The total number of elements was varied to monitor the sensitivity of the predicted temperature at a critical location within the combustion zone. Based on the convergence behavior, a mesh with 372,400 elements was selected for all subsequent simulations as it provided an optimal balance between computational cost and solution accuracy.

The present numerical model was validated against the numerical study conducted by Attia et al., which investigated non-premixed turbulent combustion of methane, methane–hydrogen mixtures, and hydrogen in a cylindrical combustion chamber using ANSYS Fluent. In their work, the authors employed the Large Eddy Simulation (LES) approach in combination with a probability density function (PDF) combustion model, and the numerical results were validated against experimental measurements.

In this study, temperature distribution was selected as the primary validation parameter, as it is a key indicator of combustion behaviour and strongly influences reaction rates and $NO_x$ formation.

The comparison of temperature profiles allows for the assessment of the predictive capability and accuracy of the present numerical model.

To ensure a meaningful and physically consistent comparison, the operating and boundary conditions adopted in the present study were closely matched to those reported by Attia et al.. These include the burner geometry, fuel composition, oxidiser ratio, inlet flow conditions, operating pressure, and combustion modelling framework. Such consistency ensures that both studies are conducted under comparable physical configurations.

Therefore, any observed discrepancies between the present results and those reported by Attia et al. can be primarily attributed to differences in numerical implementation and modelling approaches, rather than variations in physical setup or boundary conditions.

## 3. Results

### *3.1 Grid Independence and Validation Study*

The results of the grid independence study are illustrated in Figure 3. The graph shows the variation of predicted temperature against the total number of elements. It is observed that the temperature increases significantly as the mesh is refined from 140,000 to 370,000 elements. However, beyond 372,400 elements, the temperature stabilizes at approximately 820 K, with a negligible deviation (less than 0.5%) when compared to the finest mesh of 2,210,000 elements. This plateau indicates that the solution has achieved grid independence. Therefore, the medium mesh density was deemed sufficient to capture the thermal characteristics of the oxy-methane flame accurately.

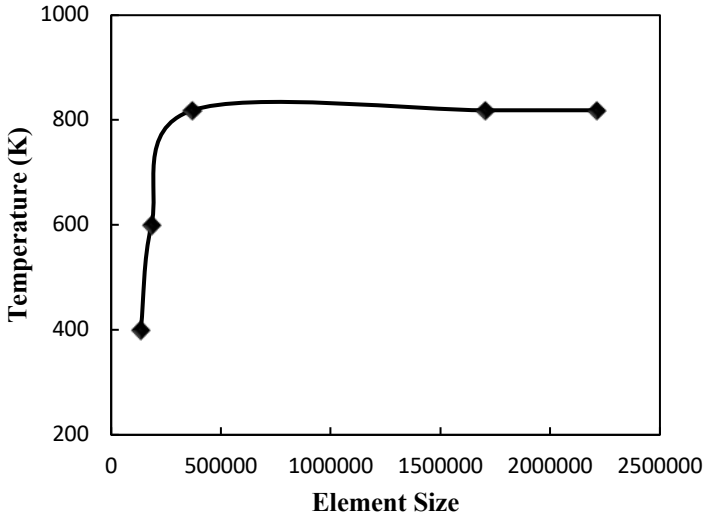


**Fig. 3.** Grid Independence study of Temperature against element size

Figure 4 compares the temperature profiles between this study and those reported by M.E.H. Attia et al. Overall, both results show good agreement along the axis of the combustion chamber. In the upstream part (around 0.05 to 0.22 m), there is a slight difference where this study predicts slightly lower temperatures than the reference. This difference is likely due to the difference in the modeling of turbulence–chemistry interactions and the numerical approach used.

In the central zone of the combustion chamber (around 0.27 to 0.80 m), both results show a very close agreement. This indicates that the developed model can accurately describe the main

combustion zone and heat release. The maximum-temperature region can also be predicted quite accurately, demonstrating the model's ability to represent the flame structure. In the downstream part (above 0.90 m), small differences are again visible, with a slight increase in error compared to other areas. This situation may be influenced by flow development, turbulence dissipation, and radiative heat transfer.

The percentage error distribution also shows that the difference between the two studies is relatively small and still within the acceptable range (less than around 10%). The lowest error is observed in the main combustion zone, while it slightly increases in the areas near the inlet and outlet. Overall, the good agreement between the results of this study and the reference data indicates that the developed numerical model can reasonably predict the temperature distribution in non-premixed oxy–methane combustion. Therefore, this model is considered validated and suitable for further analysis.

Despite the reasonable agreement with validation data, it is important to acknowledge the inherent limitations of the current numerical framework. The use of the k–omega SST RANS model provides a computationally efficient solution for steady-state furnace-scale simulations, however, it is unable to capture the transient flame dynamics and fine-scale turbulent structures that a Large Eddy Simulation (LES) could provide. Additionally, the Equilibrium Chemistry assumption used in the mixture fraction PDF approach assumes rapid reaction rates. While this is generally valid for high-temperature regions, it may slightly overlook finite-rate kinetic effects, such as local extinction or the slower oxidation of CO in highly diluted $CO_2$ environments. Future studies incorporating detailed chemical mechanisms and LES would be beneficial to further refine these localized interactions.

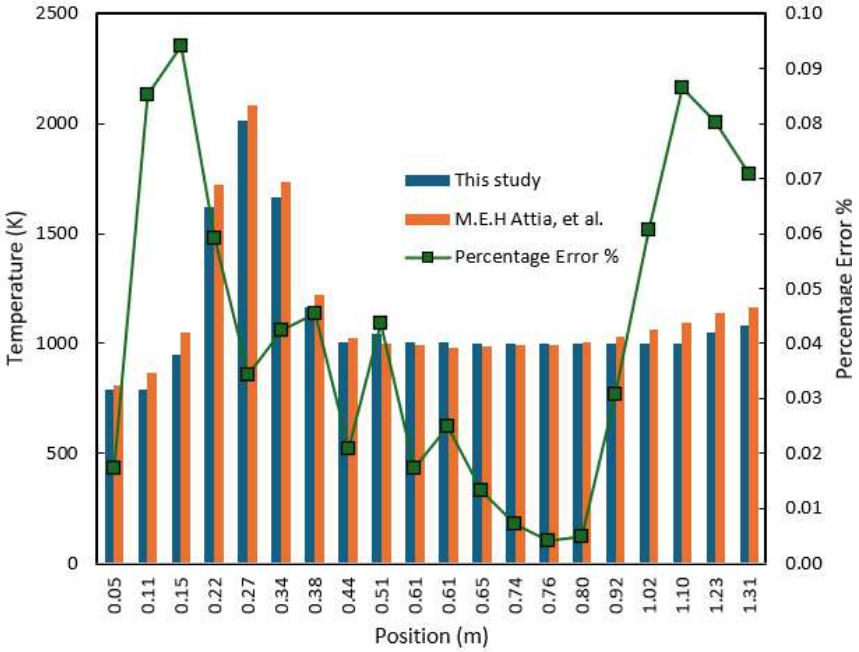


**Fig. 4.** Validation study of temperature profiles between the current study and M.E.H. Attia et al.

### *3.2 Temperature Distribution*

The temperature contours in Figure 5 show the thermal distribution for methane combustion under three oxidiser conditions: air, pure oxygen (100% $O_2$), and a diluted oxy-fuel mixture (50% $O_2$–50% $CO_2$). It can be observed that 100% $O_2$ combustion produces the highest temperature region near the burner, while air combustion exhibits a broader flame with lower peak temperature. In

contrast, the 50% $O_2$–50% $CO_2$ case shows a more diffused temperature field with reduced peak temperature and a slightly extended reaction zone.

This behaviour is mainly influenced by the dilution effects of the oxidiser composition. In the pure oxygen case, the absence of nitrogen dilution allows more chemical energy to be converted into thermal energy, resulting in higher flame temperatures. Conversely, in air combustion, the presence of nitrogen absorbs a portion of the released heat, thereby lowering the peak temperature. The addition of $CO_2$ in the oxy-fuel mixture further enhances the dilution effect due to its higher specific heat capacity and radiative properties, which reduce the overall flame temperature and broaden the heat distribution. In addition, the presence of $CO_2$ can modify the flame structure and reaction zone length, as its high heat capacity slows the reaction rate and spreads the heat release over a larger region.

This temperature distribution observed in the contour is consistent with the centreline temperature profile discussed later, where the highest temperature peak occurs near the burner for the pure oxygen case before decreasing rapidly along the axial direction.

Similar observations have been reported in recent oxy-fuel combustion studies. D. Chen et al. (2026) reported that $CO_2$ dilution significantly reduces peak flame temperature and broadens the reaction zone due to its high heat capacity and radiative properties [17]. Likewise, Liu et al. (2025) demonstrated through CFD simulations that increasing oxygen concentration in methane combustion leads to higher peak flame temperatures and more compact flame structures [18].

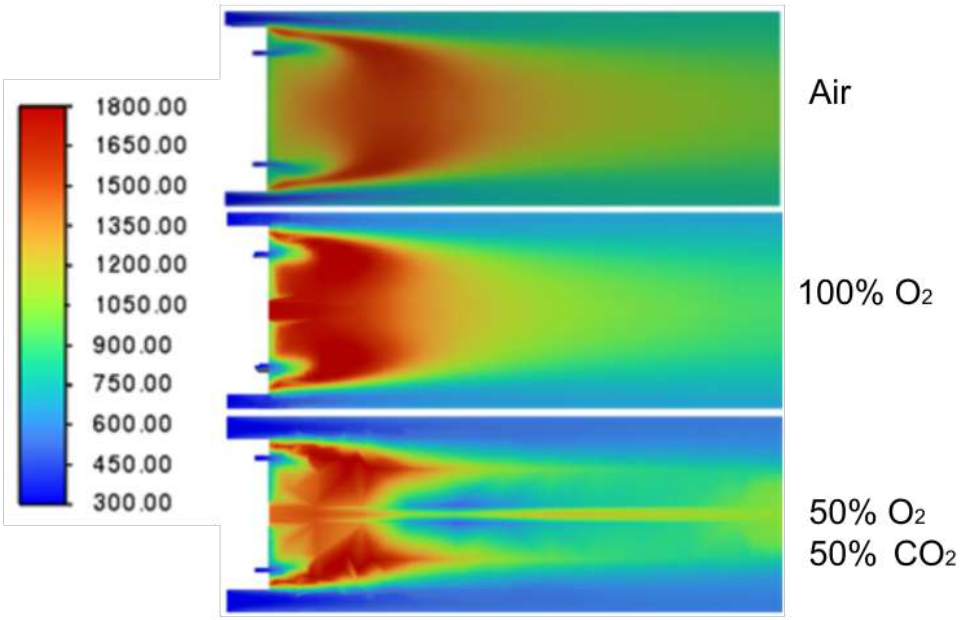


**Fig. 5.** Temperature Contour for different types of oxidiser

The centreline temperature profile shown in Figure 6 further illustrates the thermal behaviour along the combustion chamber. The graph indicates that pure oxygen combustion produces the highest peak temperature (≈1900 K) near the burner, followed by the 50% $O_2$–50% $CO_2$ mixture (≈1600 K), while air combustion exhibits a lower peak temperature of approximately 1500 K. However, further downstream, the temperature of the air combustion case becomes slightly higher than the other oxidiser conditions, indicating a slower temperature decay along the combustion chamber.

This axial trend corresponds closely with the temperature contour distribution, where the pure oxygen case shows a highly concentrated high-temperature zone near the burner while the air combustion case exhibits a longer and more distributed thermal field.

This trend occurs because pure oxygen combustion releases heat more rapidly within a short reaction zone, resulting in a sharp temperature peak followed by rapid temperature decay along the axial direction. In contrast, the presence of nitrogen in air combustion slows down the reaction rate and distributes the heat release over a longer flame region. As a result, the temperature decreases more gradually and remains relatively higher in the downstream region. The intermediate behaviour observed in the 50% $O_2$–50% $CO_2$ case suggests that $CO_2$ dilution moderates the reaction intensity while still maintaining a relatively concentrated combustion zone.

This phenomenon is consistent with recent studies on oxy-methane combustion. X. Zhang et al (2022) reported that higher oxygen concentrations produce shorter and more intense reaction zones with rapid temperature decay downstream [19]. Similarly, I.M. Machado (2020) found that $CO_2$-diluted oxy-fuel combustion results in lower peak temperatures and modified flame structures due to enhanced thermal capacity and radiative heat transfer effects [20].

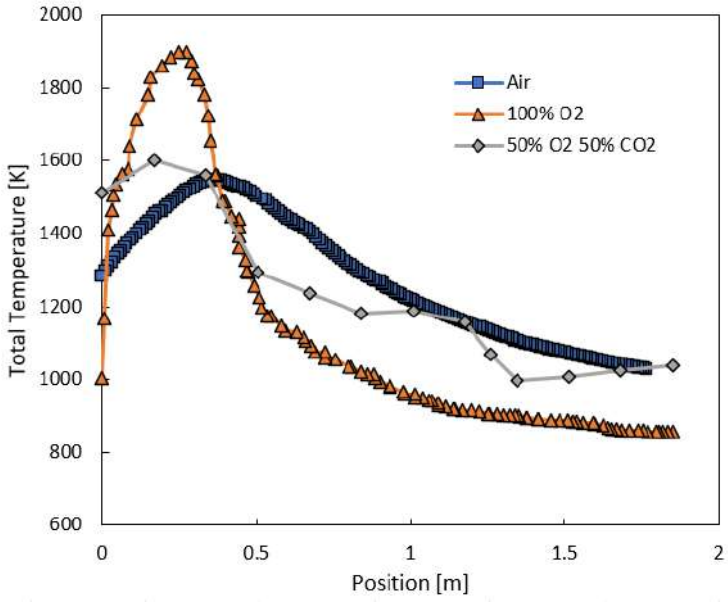


**Fig. 6.** Temperature distribution at the centerline of the combustor

### *3.3 $NO_x$, CO, CO2, O2, N2 Emissions Distribution*

The species contours in Figure 7 illustrate the spatial distribution of major combustion products and pollutants under different oxidiser conditions. Distinct variations in NO, CO, $CO_2$, $O_2$ and $N_2$ distributions can be observed depending on the oxidiser composition. The detailed quantitative behaviour of these species along the combustion chamber is further analysed using the centreline profiles presented in Figure 8. The centreline profiles of major species, including NO, CO, $CO_2$, $O_2$ and $N_2$, are presented in Figure 8 to evaluate the influence of oxidiser composition on methane combustion behaviour under different oxidising environments.

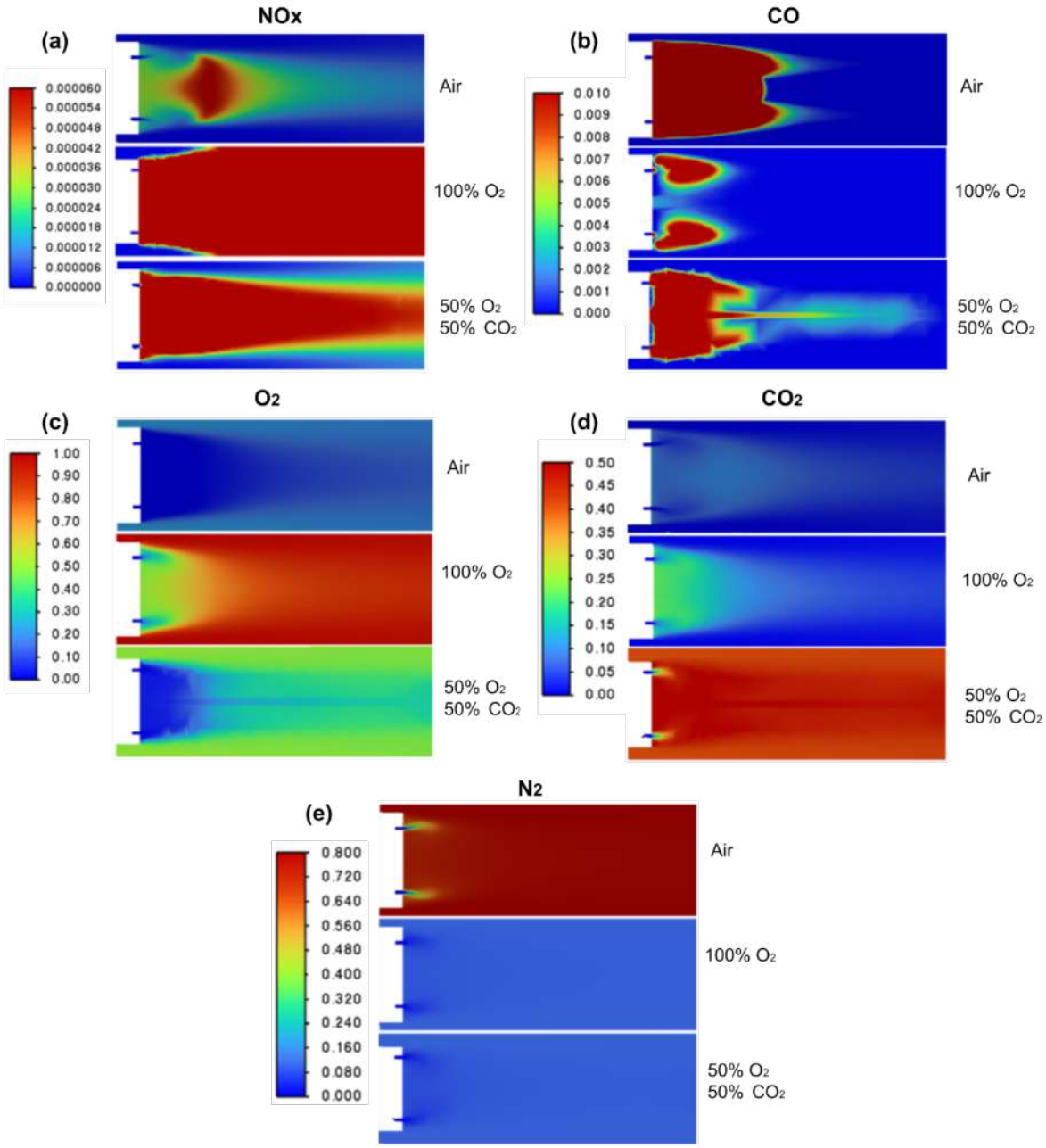


**Fig. 7.** The species contours of the spatial distribution of major combustion products and pollutants under different oxidiser conditions.

The NO mass fraction profile shows a clear variation between the three oxidiser conditions. The 100% $O_2$ combustion case produces the highest NO concentration, while air combustion exhibits significantly lower NO levels, and the 50% $O_2$–50% $CO_2$ mixture shows intermediate behaviour. This trend is mainly associated with the strong temperature dependence of thermal NO formation. As observed in the temperature analysis, pure oxygen combustion produces the highest flame temperature, which promotes NO formation through the extended Zeldovich mechanism. In contrast, nitrogen dilution in air combustion lowers the flame temperature and suppresses thermal NO formation, while $CO_2$ dilution in the oxy-fuel mixture further moderates the reaction environment. An important observation from the present results is that the pure oxygen combustion

case generates substantially higher NO compared to both air combustion and the $CO_2$-diluted oxy-fuel mixture. Although oxy-fuel combustion is often associated with reduced $NO_x$ emissions due to the elimination of atmospheric nitrogen, operating under undiluted pure oxygen conditions can instead promote thermal NO formation because of the significantly elevated flame temperatures. This highlights the critical role of $CO_2$ dilution in moderating flame temperature and controlling $NO_x$ emissions in practical oxy-fuel combustion systems. Similar behaviour has been reported in recent studies where increasing oxygen concentration significantly enhances thermal NO formation due to elevated flame temperatures [21].

The CO mass fraction profile indicates that air combustion initially produces the highest CO concentration, followed by the 50% $O_2$–50% $CO_2$ mixture, while the 100% $O_2$ combustion case produces the lowest CO concentration near the upstream region. This behaviour can be attributed to differences in combustion completeness associated with oxygen availability. In air combustion, the lower oxygen concentration caused by nitrogen dilution can lead to incomplete oxidation of carbon species, resulting in higher CO formation. In contrast, pure oxygen combustion provides sufficient oxidiser to promote more complete oxidation of intermediate species. The CO distribution therefore provides insight into combustion efficiency under different oxidiser environments. The significantly lower CO concentration observed in the pure oxygen case suggests more complete methane oxidation, as the high oxygen availability promotes the rapid conversion of CO intermediates into $CO_2$. Further downstream, however, the CO distribution shows a slight shift where the 50% $O_2$–50% $CO_2$ case exhibits marginally higher CO levels compared to air combustion, while the air case shows the lowest CO concentration in the downstream region. This behaviour may be attributed to the slower oxidation kinetics in the $CO_2$-diluted oxy-fuel mixture. The higher heat capacity of $CO_2$ reduces the local flame temperature and slows the oxidation reaction $CO + ½O_2 \rightarrow CO_2$, allowing a small amount of CO to persist further downstream. Similar trends have been reported in oxy-enriched combustion studies where $CO_2$ dilution moderates oxidation kinetics and delays complete CO conversion [22].

The $CO_2$ mass fraction distribution shows that the 50% $O_2$–50% $CO_2$ case produces the highest $CO_2$ concentration across the combustion chamber, followed by the 100% $O_2$ combustion case, while air combustion exhibits the lowest $CO_2$ concentration. This behaviour is expected because the oxy-fuel mixture already contains a significant fraction of $CO_2$ within the oxidiser stream. Consequently, the combustion products become more $CO_2$-rich compared to conventional air combustion, where nitrogen dilution significantly reduces the $CO_2$ concentration in the flue gas. The elevated $CO_2$ concentration observed in oxy-fuel combustion systems is advantageous for carbon capture and storage (CCS) applications because the flue gas stream becomes inherently rich in $CO_2$.

The $O_2$ mass fraction profile shows that pure oxygen combustion maintains the highest oxygen concentration, followed by the 50% $O_2$–50% $CO_2$ mixture, while air combustion contains the lowest oxygen fraction due to nitrogen dilution. The $O_2$ distribution also provides insight into the location of the main reaction zone within the combustion chamber. A sharp decrease in $O_2$ concentration near the burner indicates the region where methane oxidation occurs most intensely due to rapid oxygen consumption. Further downstream, the stabilisation of $O_2$ levels suggests that the majority of combustion reactions have been completed and the remaining oxygen is no longer actively involved in oxidation. This behaviour is consistent with the structure of non-premixed methane flames, where the main reaction zone is concentrated near the fuel–oxidiser mixing region.

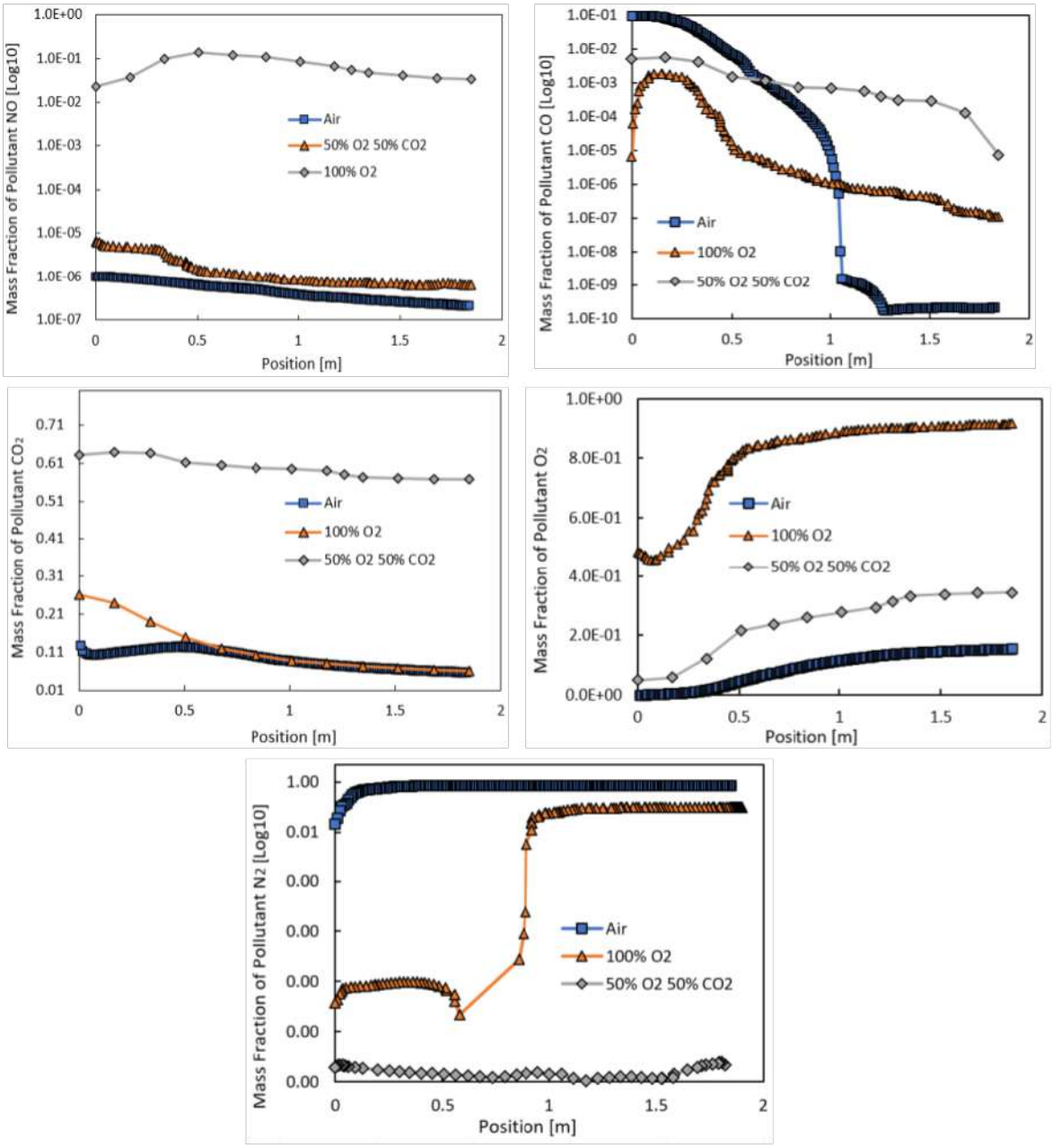


**Fig. 8.** Centreline profiles of major species, including NO, CO, $CO_2$, $O_2$ and $N_2$

The $N_2$ mass fraction profile clearly shows that air combustion produces the highest nitrogen concentration, while the 100% $O_2$ and 50% $O_2$–50% $CO_2$ cases contain significantly lower $N_2$ levels. Although the $N_2$ concentration in the 50% $O_2$–50% $CO_2$ case remains much lower than in air combustion, a slight increase in $N_2$ can be observed in the downstream region. This behaviour may be associated with minor numerical diffusion or trace nitrogen introduced through boundary conditions and mixing processes within the computational domain. Nevertheless, the overall $N_2$ concentration in the oxy-fuel cases remains negligible compared to the air combustion case, confirming that replacing air with oxygen-based oxidisers effectively eliminates nitrogen dilution in the combustion environment.

### *3.4 Velocity Distribution*

The velocity magnitude contour and centreline velocity profiles are presented in Figure 9 to evaluate the flow behaviour under different oxidiser conditions. The velocity contour indicates that the highest velocity region is concentrated near the burner inlet, where the oxidiser streams enter the combustion chamber. As the flow moves downstream, the velocity gradually decreases due to momentum dissipation and mixing between the fuel and oxidiser streams.

The centreline velocity profile shows that air combustion produces the highest velocity near the upstream region, followed by the 50% $O_2$–50% $CO_2$ mixture, while the 100% $O_2$ case exhibits the lowest velocity magnitude. This behaviour is primarily related to the differences in gas density and volumetric flow characteristics of the oxidiser streams. Air contains a large fraction of nitrogen which increases the total volumetric flow rate, resulting in higher inlet velocity compared to the oxygen-based oxidisers.

A rapid drop in velocity is observed within the first 0.2–0.3 m, which corresponds to the primary mixing region where strong interaction between methane and oxidiser occurs. This region is typically associated with the main combustion zone, where chemical reactions and heat release significantly alter the flow field.

Further downstream, the velocity gradually increases and stabilises as the combustion process approaches completion and the flow becomes more uniform along the chamber. In this region, the air combustion case maintains slightly higher velocity compared to the oxy-fuel cases, while the 50% $O_2$–50% $CO_2$ mixture shows the lowest velocity magnitude, which can be attributed to the higher molecular weight and density of $CO_2$ in the oxidiser mixture.

When the velocity behaviour is considered together with the temperature and species distributions, the results indicate that the air combustion case promotes stronger mixing due to higher flow momentum, whereas the oxy-fuel cases exhibit more controlled mixing environments that influence flame temperature and species formation. This interaction between flow dynamics, heat release and chemical reactions plays an important role in determining flame stability and pollutant formation characteristics within the combustor.

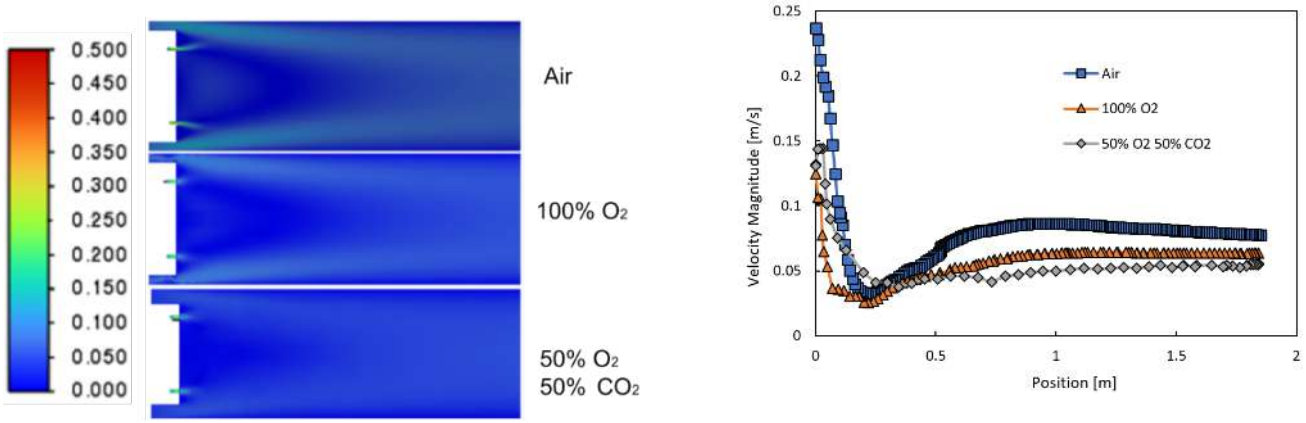


**Fig. 9.** The velocity magnitude contour and centreline velocity profiles

### *3.5 Overall Performance of Single-Stage Combustion under Different Oxidiser Conditions*

A summary of the thermal and emission characteristics of methane combustion under the investigated oxidiser environments is presented in Table 4.1. From the results, it can be observed that the air-fired configuration produces a more moderated thermal profile, with peak temperatures

in the range of 1700–1750 K. This behaviour is largely influenced by the presence of nitrogen, which acts as an inert diluent, reducing the overall reaction intensity and suppressing the formation of thermal $NO_x$.

In contrast, the case with 100% O2 shows the highest thermal intensity, with peak temperatures reaching approximately 1800 K. This increase in temperature is accompanied by a noticeable rise in $NO_x$ emissions. Such behaviour suggests that under oxygen-enriched conditions, the higher heat release rate tends to intensify the thermal $NO_x$ formation mechanism.

On the other hand, the 50% O2 – 50% CO2 mixture exhibits an intermediate combustion behaviour. The presence of CO2 plays an important role as a thermal diluent, mainly due to its relatively high heat capacity. This helps to moderate the combustion temperature and, at the same time, reduce $NO_x$ formation when compared to the pure oxygen case. As a result, this configuration offers a more balanced performance between combustion intensity and emission control.

**Table 2**
Summary of peak temperature and $NO_x$ emissions for single-stage combustion under different oxidiser conditions

| Case | Peak | NOx | Fundamental Interpretation |
|---|---|---|---|
| Air Oxidiser | 1700–1750 | Lowest | N2 acts as an inert diluent, suppressing reaction intensity and thermal NOx kinetics. |
| 50% O2 – 50% CO2 | 1800 | Moderate | CO2 provides enhanced thermal dilution, regulating combustion through higher specific heat capacity. |
| 100% O2 | 1800 | Highest | Oxygen enrichment accelerates heat release, |

## 4. Conclusions

This study presents a detailed numerical analysis of non-premixed methane combustion under several oxidizer configurations, using the k–ω Shear Stress Transport (SST) turbulence model in the RANS framework. The reliability of the model was assessed by comparison with experimental data and previous simulation results, where the average error obtained was less than 10% for the predicted temperature distribution. The numerical uncertainty was minimized through a grid independence study, resulting in a discretization error of less than 0.5% for the peak temperature, while model sensitivity was managed using the robust k-ω SST framework which is less sensitive to ambient turbulence properties. Based on the analysis carried out, some key observations can be summarized as follows.

From the thermal profile and flame structure point of view, the use of pure oxygen (100% $O_2$) produces a more concentrated reaction zone with a high peak temperature, which is around 1900 K. When $CO_2$ is introduced as a diluent at a rate of 50% in the oxy-fuel system, the peak temperature is found to decrease to about 1600 K, while the reaction zone becomes wider. This change is closely related to the high specific heat capacity of $CO_2$ and its irradiance properties, which affect the heat transfer pattern in the combustion chamber.

Regarding the mechanism of NOx formation, the study findings showed that the use of pure oxygen, although increasing the combustion intensity, also contributed to a sharp increase in thermal NOx. This situation occurred through the Zeldovich mechanism which is very sensitive to high temperatures. On the other hand, a mixture of 50% $O_2$ and 50% $CO_2$ was found to be more effective in controlling NOx formation, without significantly affecting flame stability.

From the perspective of carbon monoxide (CO) kinetics and combustion efficiency, conventional air combustion shows higher CO formation in the early stages. This phenomenon is attributed to the

nitrogen dilution effect that limits the local oxygen availability. Although the use of 100% $O_2$ accelerates the CO oxidation in the upstream section, the presence of CO2 in the oxy-fuel system was found to slow down the $CO+1/2O_2 \rightarrow CO_2$ reaction rate in the downstream section, which is influenced by the thermal effect of the gas.

This numerical study is not limited to standard parameter comparisons but demonstrates the strategic necessity of $CO_2$ dilution in transitional combustion systems. Based on the specific 50% $O_2$ – 50% $CO_2$ configuration investigated in this study, the findings of this study conclude that a critical trade-off occurs; while pure oxy-methane combustion maximizes thermal intensity, reaching approximately 1900K, it also creates an unsustainable environment for conventional material durability and leads to aggressive thermal NOx kinetic production via the Zeldovich mechanism.

The use of 50% $CO_2$ acts as a thermal buffer, where its high heat capacity and radiative properties help lower the flame temperature to approximately 1600 K without compromising flame stability. From an engineering perspective, this configuration represents an 'integrated-capture' design rather than merely an add-on system after combustion. This provides a practical operational guideline and an optimal operational window to maintain equipment longevity through lower peak temperatures, while producing a high-$CO_2$ exhaust gas ready for the CCS process. Finally, $CO_2$ recirculation is proven to be not just a common diluent agent, but a key control variable to balance combustion performance with global decarbonization goals.

To build upon the current findings, future research should include parametric studies investigating a broader range of $CO_2$ dilution ratios, such as 20% to 80%, to further detail the sensitivity of NOx formation to various dilution levels. Furthermore, the application of Large Eddy Simulation (LES) is suggested to capture the transient flame dynamics and fine-scale turbulent interactions that were not fully resolved in this steady-state RANS framework.

**Acknowledgement**
This research was supported by Universiti Tun Hussein Onn Malaysia (UTHM) through Tier 1 (vot Q969).

**Conflict of Interest Statement**
The authors declare that there is no conflict of interest regarding the publication of this paper. No financial support, grants, or other forms of compensation were received that could have influenced the outcomes of this work. The research was conducted in the absence of any commercial or financial relationships that could be construed as a potential conflict of interest.

**Author Contributions Statement**
**Nur Atiqah Habib** conducted the CFD simulations, performed data analysis, and wrote the initial draft of the manuscript. **Nor Afzanizam Samiran** conceptualized and designed the study, supervised the project, and reviewed the manuscript. **Izuan Amin Ishak**, **Rais Hanizam Madon**, and **Nik Normunira Mat Hassan** contributed to data interpretation and manuscript revision. All authors have read and approved the final version of the manuscript.

**Data Availability Statement**
All data generated or analyzed during this study are included in this published article. Additional datasets regarding the numerical simulations are available from the corresponding author upon reasonable request.

**Ethics Statement**

This study was conducted in accordance with the ethical standards of the institutional and national research committee. As this research involved numerical modeling and simulation, no human or animal participants were involved, and informed consent was not required.

**References**

[1] Ertesvåg, Ivar S., Paweł Madejski, Paweł Ziółkowski, and Dariusz Mikielewicz. "Exergy Analysis of a Negative Co2 Emission Gas Power Plant Based on Water Oxy-Combustion of Syngas from Sewage Sludge Gasification and Ccs." *Energy* 278 (2023). https://doi.org/10.1016/j.energy.2023.127690.

[2] Greencorn, Michael J., S. David Jackson, Justin S. J. Hargreaves, Souvik Datta, and Manosh C. Paul. "Thermodynamic Limitations to Direct Co2 Utilisation within a Small-Scale Integrated Biomass Power Cycle." *Energy Conversion and Management* 269 (2022). https://doi.org/10.1016/j.enconman.2022.116144.

[3] Marzouk, O. A. "Estimated Electric Conductivities of Thermal Plasma for Air-Fuel Combustion and Oxy-Fuel Combustion with Potassium or Cesium Seeding." *Heliyon* 10, no. 11 (Jun 15 2024): e31697. https://doi.org/10.1016/j.heliyon.2024.e31697. https://www.ncbi.nlm.nih.gov/pubmed/38832275.

[4] Wang, Zhichao, and Xiaoyi Yang. "Nox Formation Mechanism and Emission Prediction in Turbulent Combustion: A Review." *Applied Sciences* 14, no. 14 (2024). https://doi.org/10.3390/app14146104.

[5] Türkkahraman, Zeliha, and Buğrahan Alabaş. "Effect of Oxy-Fuel Combustion on Temperature, Flame Speed and Nox Emission Values of Methane-Ammonia Flames in a Model Gas Turbine Combustor." *Fuel* 422 (2026). https://doi.org/10.1016/j.fuel.2026.139138.

[6] Al-Mrayatee, Hussein M., Reyadh Ch Al-Zuhairy, and Dhamyaa S. Khudhur. "Cfd Study of Flame Characteristics in Oxy-Fuel Combustion under Different $O_2/Co_2$ Ratios." *International Journal of Heat and Technology* 43, no. 6 (2025): 2413-23. https://doi.org/10.18280/ijht.430637.

[7] Mubashir, Muhammad, Dekui Shen, Muhammad Aurangzeb, Sheeraz Iqbal, Md Shafiullah, Aymen Flah, and Habib Kraiem. "Cfd-Guided Catalytic Combustion Optimization of Ch4/H2/Nh3 Blends Using Staged Ni-Based Catalysts: Insights into Nox Mitigation and Efficiency Enhancement." *Fuel Processing Technology* 277 (2025). https://doi.org/10.1016/j.fuproc.2025.108315.

[8] Ren, Shoujun, and Xiaohan Wang. "No Emission and Its Reduction Mechanism Investigation in One Diffusion-Like Vortex-Tube Combustor." *Journal of Cleaner Production* 274 (2020). https://doi.org/10.1016/j.jclepro.2020.123138.

[9] Sun, Zhijun, Qining Wu, Chenxu Zhao, Haixia Li, and Anchao Zhang. "A Review of Nox Control by Mild-Oxy Combustion." *Journal of the Energy Institute* 113 (2024). https://doi.org/10.1016/j.joei.2023.101502.

[10] Hajivand, Masoud. "High-Fidelity Rans Cfd Simulations of Physico-Chemical Process of Combustion in Gas Turbine Combustion Chambers in Ansys Cfx." *Energy engineering and control systems* 10, no. 2 (2024): 81-95. https://doi.org/10.23939/jeecs2024.02.081.

[11] Ke, Enlei, Chenzhen Ji, Mengming Wang, Deng Pan, and Tong Zhu. "Prediction of Flame Transfer Function and Combustion Instability on a Partially Premixed Swirling Combustor by the System Identification and Cfd Methods." *Aerospace Science and Technology* 151 (2024). https://doi.org/10.1016/j.ast.2024.109275.

[12] Firooznia, Neda, and Cyrus Aghanajafi. "Numerical Simulation and Pso-Based Analysis of $No_x$, Co, and $Co_2$ Emissions in Mild Combustion of Methane/Ammonia/Hydrogen Blends with Steam Addition." *Results in Engineering* 28 (2025). https://doi.org/10.1016/j.rineng.2025.107741.

[13] Jeon, Ki Tae, and Jong Guen Lee. "Effect of Fuel/Oxidizer Mixing on Combustion Efficiency for Co2-Diluted Methane Oxy-Flames and Methane/Air Flames." *Fuel* 422 (2026). https://doi.org/10.1016/j.fuel.2026.139173.

[14] Daurer, Georg, Stefan Schwarz, Martin Demuth, Christian Gaber, and Christoph Hochenauer. "Evaluation of Numerical Modeling and Combustion Characteristics of Hydrogen Oxy-Fuel Combustion in a Semi-Industrial Furnace." *Fuel* 369 (2024). https://doi.org/10.1016/j.fuel.2024.131690.

[15] Gu, Jinrao, Qinwen Liu, Wenqi Zhong, and Aibing Yu. "Study on Scale-up Characteristics of Oxy-Fuel Combustion in Circulating Fluidized Bed Boiler by 3d Cfd Simulation." *Advanced Powder Technology* 31, no. 5 (2020): 2136-51. https://doi.org/10.1016/j.apt.2020.03.007.

[16] Kislinger, Christian, Georg Daurer, Gabriel Manier, Jean-Charles Boullot, Stefan Schwarz, Martin Demuth, Christian Gaber, and Christoph Hochenauer. "Detailed Cfd Study of Air–Fuel, Oxygen-Enriched and Partial Oxy-Fuel Combustion with Optimized Fuel Savings in an Industrial Reheating Furnace." *Applied Thermal Engineering* 291 (2026). https://doi.org/10.1016/j.applthermaleng.2026.130276.

[17] Chen, Dengke, Chang Xing, Rongze Ma, Penghua Qiu, Yijun Zhao, Jingyu Guan, Rui Sun*, et al.* "Thermal Versus Chemical Effects of Co2 Dilution on Micro-Mixing Flame and No Emission." *Fuel* 407 (2026). https://doi.org/10.1016/j.fuel.2025.137267.

[18] Liu, Junlong, Zhancheng Dou, Yujuan Li, Xingdong Su, Jinfang Yao, Wenlong Dong, and Huaqiang Chu. "Numerical Study on Soot Formation in Methane/<I>N</I>-Heptane Laminar Diffusion Flames under an Oxygen-Rich Environment at Elevated Pressure." *Progress in Reaction Kinetics and Mechanism* 50, no. 1 (2025): 0-0. https://doi.org/10.48130/prkm-0025-0023.

[19] Zhang, Xiao, Yitong Duan, Ren Zhang, Haiqiao Wei, and Lin Chen. "Optical Study of Oxygen Enrichment on Methane Combustion Characteristics under High Compression-Ratio Conditions." *Fuel* 328 (2022). https://doi.org/10.1016/j.fuel.2022.125251.

[20] Machado, I. M., P. Pagot, and F. M. Pereira. "Experimental Study of Radiative Heat Transfer from Laminar Non-Premixed Methane Flames Diluted with Co2 and N2." *International Journal of Heat and Mass Transfer* 158 (2020). https://doi.org/10.1016/j.ijheatmasstransfer.2020.119984.

[21] Wei, Yi, Zunhua Zhang, Mengni Zhou, Dongsheng Dong, Weiping Yu, Xiaoxiong Mi, and Gesheng Li. "Effects of Ambient Oxygen Concentrations on Pollutants Formation in Premixed Natural Gas Ignited by Pilot Diesel Spray: Large-Eddy Simulations." *Fuel* 371 (2024). https://doi.org/10.1016/j.fuel.2024.132057.

[22] Cheng, Gang, Haiyan Wang, Bo Tan, and Shuhui Fu. "Carbon Dioxide Prevents Oxygen Adsorption at Low-Temperature Oxidation Stage of Low-Rank Coal: Laboratory Study and Molecular Simulation." *Processes* 11, no. 8 (2023). https://doi.org/10.3390/pr11082504.